

Friedel phases and phases of transmission amplitudes in quantum scattering systems

Tooru Taniguchi and Markus Büttiker

Département de Physique Théorique, Université de Genève, CH-1211, Genève 4, Switzerland

(Received 30 June 1999)

We illustrate the relation between the scattering phase appearing in the Friedel sum rule and the phase of the transmission amplitude for quantum scatterers connected to two one-dimensional leads. Transmission zero points cause abrupt phase changes $\pm\pi$ of the phase of the transmission amplitude. In contrast, the Friedel phase is a continuous function of energy. We investigate these scattering phases for simple scattering problems and illustrate the behavior of these models by following the path of the transmission amplitude in the complex plane as a function of energy. We verify the Friedel sum rule for these models by direct calculation of the scattering phases and by direct calculation of the density of states. [S0163-1829(99)06343-2]

I. INTRODUCTION

The phase is an essential concept in quantum scattering theory. Some key results and techniques, such as partial-wave expansion,¹ and the Friedel sum rule² depend in an explicit manner on the scattering phase. The Friedel sum rule connects the density of states to the charge (or a charge difference) of the system via the phase of the eigenvalues of the scattering matrix.²⁻⁵ Since the Friedel phase is related to the density of states, it is also connected to thermodynamic statistical mechanics quantities^{5,6} such as the persistent current.⁷ In addition to the total density of states, the scattering phases also play an important role in the partial density of states⁸ (density of states with a preselection or postselection of the incident or exiting quantum channel) and in transport coefficients such as capacitances⁹ and charge relaxation resistances.¹⁰

The principal aim of this work is to investigate the behavior of the phase in simple scattering problems as they frequently occur in mesoscopic physics. In particular, we would like to understand which phases are continuous functions of external parameters (Fermi energy, magnetic field, or Aharonov-Bohm flux) and which phases are permitted to exhibit jumps as a function of the external parameters. We consider coherent quantum scattering systems connected to two semi-infinite, one-channel leads in the absence of a magnetic field and without spin-orbit scattering. Consider, for instance, the transmission amplitude t , which determines the transmitted current amplitude if there is an incident current of unit amplitude. The transmission amplitude can be expressed in terms of its modulus $|t|$ and its phase $\theta^{(t)}$,

$$t \equiv |t| e^{i\theta^{(t)}}. \quad (1)$$

If, as a function of energy, $|t|$ is always positive, the path of the transmission amplitude will encircle the origin of the complex plane but always stay at a finite distance from it. An example of such a behavior is shown in Fig. 1. As a consequence, the phase $\theta^{(t)}$ is a continuous function of the energy. If, on the other hand, $|t|$ is zero for a certain value of the external parameter, the path of the transmission amplitude in the complex plane will necessarily pass through the origin. As a consequence, the phase $\theta^{(t)}$ will jump at this energy by

π . Such a behavior is shown in Fig. 2. A specific model giving rise to the behavior shown in Fig. 1 is the transmission amplitude of a simple one-dimensional resonant tunnel barrier structure. The transmission probability never vanishes, and the phase $\theta^{(t)}$ is a continuous function of energy that increases in each complete revolution by 2π . In contrast, Fig. 2 shows the transmission amplitude for a simple model of a side branch of finite length attached to a perfect wire. The transmission amplitude as a function of energy passes through zero, and the phase that increases by π through each revolution also exhibits a jump of π (or $-\pi$) bringing the phase back to its origin.

The two models with the very distinctive behavior can be combined, and the evolution of the transmission amplitude of such a combined model is shown in Fig. 3. Now the graph shows very many revolutions through the origin and occasionally a revolution around the origin. We believe that this reflects the generic behavior of the transmission amplitude in the complex plane.

Obviously, the phase of the transmission amplitude in the second example, Fig. 2, since it is not a continuous function, cannot play the role of the scattering phase, which is used in the Friedel sum rule. For a system with a density of states ρ , there must exist a phase that we denote by $\theta^{(f)}$ and which we call the *Friedel phase*, such that its energy derivative is directly related to the density of states

$$\frac{\partial \theta^{(f)}}{\partial E} = \pi \rho. \quad (2)$$

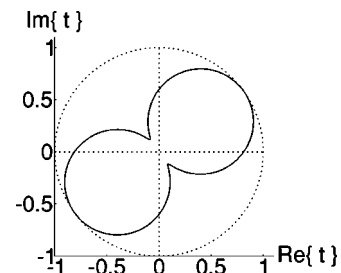


FIG. 1. Transmission amplitude as a function of energy for a resonant double-barrier.

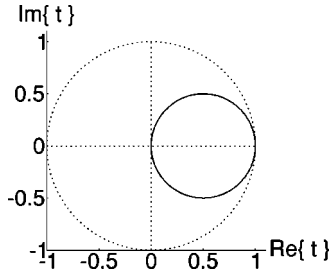


FIG. 2. Transmission amplitude as a function of energy for a wire with a side branch.

Since the density of states should be a continuous function of the energy for the scattering problems we have in mind, the Friedel phase must also be a continuous function of energy. One aim of our work is to investigate and illustrate the behavior of the different phases $\theta^{(t)}$ and $\theta^{(f)}$ and to investigate their connection to the scattering matrix of the problem.

The problem investigated here is of interest in connection with the experiments of Yacoby *et al.*,¹¹ and Schuster *et al.*¹² In the experiment of Yacoby *et al.*, an Aharonov-Bohm ring with a quantum dot was investigated in a two terminal geometry. In a two terminal geometry, the Aharonov-Bohm effect exhibits a *parity*:¹³ As a function of the Aharonov-Bohm flux, the conductance is either a local minimum at zero flux (positive parity) or a local maximum (negative parity). In the experiment of Yacoby *et al.*, it was observed that over a sequence of more than a dozen Coulomb blockade peaks the parity changes at each peak in an identical manner. It is observed that the parity is positive to the left of the Coulomb blockade peak and negative to the right of the Coulomb blockade peak. Such a behavior is incompatible with a simple resonant tunneling model (Fig. 1) but would be in accordance with the evolution of the transmission amplitude shown in Fig. 2. The second important experimental fact is that the phase drops by π between Coulomb blockade peaks as shown in the experiment of Schuster *et al.* Again, this behavior is compatible with Fig. 2 but not with Fig. 1. A number of efforts^{13–28} have been made to explain the fact that the behavior of the parity is the same at each peak. Reference 13 suggested a screening effect, Ref. 15 alluded to degeneracies, and Refs. 17, 20, 21, and 24 proposed asymmetric deformation of the dot and repeated tunneling through exactly the *same* state. The same mechanism due to a dot that is only semichaotic is supported by Silvestrov and Imry²⁸ who point to the large variation in the lifetime of states in a semichaotic dot. Reference 29 proposes that co-

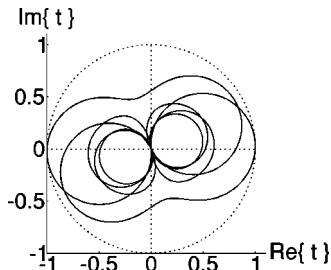


FIG. 3. Transmission amplitude as a function of the particle energy for a model that combines the resonant tunnel barrier and the side branch.

tunneling involving several levels might generate interaction induced correlations between the parity observed at subsequent peaks. A possible role of zero's of the transmission probability, Fig. 2, was suggested to us in informal communication by Levy Yeyati³⁰ and has since found interest in a number of works.^{18,22,23,25–27} We mention here especially the work by Ryu and Cho²³ who investigate an *AB* ring with a dot that is also connected to a side branch. Apart from Ref. 13, the Friedel sum rule has thus far only found interest in the recent work of Lee.²⁷ The work presented here is in very close connection to the paper by Ryu and Cho and the paper by Lee.

It is possible that the experimental observation of identical behavior over many subsequent conductance peaks is in fact generic (i.e., is observed for a fully chaotic quantum dot) and does not require a system with special properties that generates tunneling through the same state. The parity of the Aharonov-Bohm effect was observed in a multichannel GaAs ring already almost a decade ago in an experiment by Ford *et al.*³¹ In this experiment the ring is coupled to a back gate, and the experiment shows wide regions in the gate voltage – magnetic-field plane in which the parity of the Aharonov-Bohm effect remains the same.

In this work we investigate the various phases of the scattering matrix and their relation to the phase of the transmission amplitude $\theta^{(t)}$ and the Friedel phase $\theta^{(f)}$ comparing in detail two simple model systems, a one-dimensional resonant tunneling problem and a perfect wire with a side branch, and briefly discuss also the combination of these two models.

II. FRIEDEL PHASE AND TRANSMISSION AMPLITUDE PHASE

We consider systems connected to two semi-infinite, one-dimensional leads. The system itself can be a multidimensional, i.e., a quantum dot. We consider phase-coherent scattering and neglect particle-particle interactions and inelastic-scattering effects. In such systems the scattering matrix S in the particle energy E is represented as a 2×2 matrix in which S_{jj} is the reflection amplitude back into the j th lead for carriers incident in the j th lead ($j=1,2$), and S_{jk} is the transmission amplitude from the k th lead to the j th lead ($j \neq k$, $j=1,2$, and $k=1,2$). The scattering matrix is a unitary matrix, $S^{-1} = S^\dagger$. This condition guarantees a conservation of the particle current. Furthermore, it implies that the eigenvalues of the scattering matrix S are on the unit circle. Therefore, the eigenvalue of the scattering matrix S can be represented as $\exp(2i\xi_j)$ with a real quantity ξ_j ($j=1,2$). Below, we show that we obtain the Friedel sum rule if we define the *Friedel phase* $\theta^{(f)}$ by

$$\theta^{(f)} \equiv \sum_{j=1}^2 \xi_j. \quad (3)$$

As for any definition of a phase, Eq. (3) defines the Friedel phase only up to a multiple of π . A unitary 2×2 matrix can be parametrized as

$$S = \begin{pmatrix} i e^{i(\theta + \varphi_1)} \sin \phi & e^{i(\theta + \varphi_2)} \cos \phi \\ e^{i(\theta - \varphi_2)} \cos \phi & i e^{i(\theta - \varphi_1)} \sin \phi \end{pmatrix} \quad (4)$$

with real phases θ , φ_1 , φ_2 , and ϕ . The eigenvalues of this matrix $\exp(2i\xi_j)$ are determined by

$$\sin(2\xi_j - \theta) = \sin \varphi_1 \cos \phi. \quad (5)$$

The eigenvalues are independent of φ_2 . Furthermore, if ξ_- is a solution of Eq. (5), then a second solution is $2\xi_+ - \theta = \pi - (2\xi_- - \theta)$. Consequently, the sum of the two phases of these eigenvalues is $2\xi_+ + 2\xi_- = \pi + 2\theta$. Thus, according to Eq. (3), the Friedel phase is given by

$$\theta^{(f)} = \theta + \frac{\pi}{2}. \quad (6)$$

Apart from a constant $\pi/2$, the Friedel phase is determined only by the phase θ of the scattering matrix. In particular, as also emphasized by Lee,²⁷ it would be incorrect to identify the Friedel phase with the argument of the transmission amplitude.

The derivative of the Friedel phase $\theta^{(f)}$ with respect to the particle energy E can be related to the energy derivatives of the scattering matrix. The density of states can also be expressed in terms of the scattering matrix.⁵ This gives us a relation that connects the energy derivative of the Friedel phase and the scattering matrix with the density of states,

$$\frac{\partial \theta^{(f)}}{\partial E} = \frac{1}{4i} \sum_{j=1}^2 \sum_{k=1}^2 \left(S_{jk}^* \frac{\partial S_{jk}}{\partial E} - \frac{\partial S_{jk}^*}{\partial E} S_{jk} \right) = \pi \rho. \quad (7)$$

Integration of this relation over the energy interval $[E_1, E_2]$ gives the Friedel sum rule, which thus states that the difference in phase $\theta^{(f)}(E_2) - \theta^{(f)}(E_1)$ is equal to the number of particles $N(E_2, E_1)$ multiplied by π in the system in this energy interval,

$$\theta^{(f)}(E_2) - \theta^{(f)}(E_1) = \pi N(E_2, E_1). \quad (8)$$

The Friedel phase is thus a *continuous* function of energy (either E_2 or E_1) since the density of states is a continuous function of energy.

Another phase that is frequently discussed is the argument $\theta^{(t)}$ of the transmission amplitude defined by Eq. (1). Below, we will consider only systems with time-reversal invariance. For such systems, the scattering matrix is symmetric $S_{12} = S_{21}$, and consequently, $\varphi_2 = 0$ or $\varphi_2 = \pi$. To be definite, we take $\varphi_2 = 0$. In this case the phase of the transmission amplitude is given by

$$\theta^{(t)} = \theta + \pi \Theta(\cos \phi), \quad (9)$$

where $\Theta(x)$ is the step function of x . In contrast to the Friedel phase, the phase of the transmission amplitude is thus, in general, not a continuous function of energy but exhibits a jump of π when $\cos \phi$ changes sign. The Friedel phase and the transmission amplitude phase are not completely independent. From Eqs. (6) and (9) we find

$$\theta^{(t)} = \theta^{(f)} - \frac{\pi}{2} + \pi \Theta(\cos \phi). \quad (10)$$

Differentiating Eq. (10) with respect to energy (or any other variable of interest) we find

$$\Delta \theta^{(t)} = \Delta \theta^{(f)} + \pi \delta(\cos \phi) \Delta \cos \phi, \quad (11)$$

where we have used the abbreviation $\Delta = \partial/\partial E$. Equation (11) shows that only if the condition $\cos \phi \neq 0$ is satisfied for all values of the parameters is the phase of the transmission amplitudes equal to the Friedel phase. The condition $\cos \phi \neq 0$ means that the transmission probability $|t|^2$ is nowhere equal to zero. Therefore, it is the existence of zero points of the transmission probability that is at the origin of the difference of the Friedel phase and the phase of the transmission amplitude.

To be more precise, in addition to a zero point in the transmission probability, it is also required that the energy derivative of $\partial \cos \phi/\partial E$ is nonzero at the transmission zero-points. To see this, we consider phase changes due to the energy E only and assume that the number of zero points of the transmission probability is finite or countable. The zero points of the transmission probability determine a sequence of energies that we denote by $E^{(n)}$, $n = 1, 2, \dots$. Using Eqs. (7) and (11), we obtain

$$\frac{\partial \theta^{(t)}}{\partial E} = \pi \rho + \pi \sum_n \operatorname{sgn} \left(\left. \frac{\partial \cos \phi}{\partial E} \right|_{E=E^{(n)}} \right) \delta(E - E^{(n)}), \quad (12)$$

where the function $\operatorname{sgn}(x)$ of x is the sign function. It may be noted that the second term of the right-hand side of Eq. (12) is zero even at a transmission zero point if $\partial \cos \phi/\partial E$ is zero at such a point. However, we expect that such cases are unlikely, and we proceed by assuming that $\partial \cos \phi/\partial E$ is not zero at any transmission zero point.

To summarize, the Friedel phase is a continuous function of energy. On the other hand, the argument of the transmission amplitude might exhibit jumps. These conclusions agree with Lee.²⁷

III. EVOLUTION OF THE PATH OF THE TRANSMISSION AMPLITUDE CONNECTING CONSECUTIVE RESONANCES

We now discuss, from a general point of view, the conditions that lead to the behavior shown in Figs. 1, 2, and 3. We consider a set of parameters for which the transmission probability shows a series of peaks as function of energy. We now ask: What portion of the path of the transmission amplitude shown in Fig. 1 and Fig. 2 is traced out if we increase the energy from its value at a peak in the transmission probability to a value corresponding to the subsequent peak in the transmission probability? Let us denote the energy of the n th peak in the transmission probability by \mathcal{E}_n . In addition, let us consider the condition

$$\int_{\mathcal{E}_n}^{\mathcal{E}_{n+1}} dE \quad \rho \sim 1, \quad (13)$$

which according to the Friedel sum rule implies that one particle is added to the scattering region. Using this condition and integrating both sides of Eq. (12) with respect to the energy from \mathcal{E}_n to \mathcal{E}_{n+1} , we find

$$\theta^{(t)}(\mathcal{E}_{n+1}) - \theta^{(t)}(\mathcal{E}_n) \sim \begin{cases} \pi & \text{case A} \\ 0 \text{ or } 2\pi & \text{case B.} \end{cases} \quad (14)$$

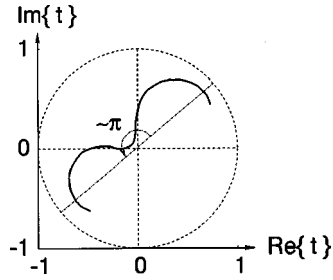


FIG. 4. Schematic representation of the path of the transmission amplitude as a function of the particle energy for the case that there is no transmission zero. The energy interval covered is that needed for the transition from one resonant peak (in the transmission probability) to the next resonant peak. The phase changes by about π .

In case *A* there is no transmission zero point in the energy interval $(\mathcal{E}_n, \mathcal{E}_{n+1})$, and in case *B* there is a transmission zero point in the energy interval $(\mathcal{E}_n, \mathcal{E}_{n+1})$. In case *A* the phase $\theta^{(t)}$ evolves by π through the consecutive resonant peaks, so that the resulting path of the transmission amplitude is as shown in Fig. 4. On the other hand, in case *B* the phase $\theta^{(t)}$ of the transmission amplitude increases by 2π (or 0) between the consecutive resonant peaks, so that the trace of the transmission amplitude is as shown in Fig. 5.

It is clear that Fig. 1 is composed of two paths of the type shown in Fig. 4, and Fig. 2 is the result of a path of the type shown in Fig. 5. Consequently, there is a profound difference in the behavior of these two systems: Whereas, for instance, in a double-barrier scattering problem, we need to increase the energy over two consecutive states to rearrive at the starting point, for the wire with a side branch an energy increase over one state only is sufficient to bring the system back to the same point. We also remark that Fig. 3 is composed of combinations of the paths shown in Figs. 4 and 5.

Clearly, it would be desirable to classify all the possible paths that are taken in the complex plane as we proceed from one transmission peak to another. Here we have emphasized only two paths, namely those shown in Figs. 4 and 5. These two possibilities are direct consequences of the condition (13), but, of course, there might exist scattering problems that do not obey this condition.

To summarize this section, we have shown that the addition of a particle to the system can lead to at least two very distinct paths of the transmission amplitude in the complex plane. For paths of type *A* (see Fig. 4), the parity of the

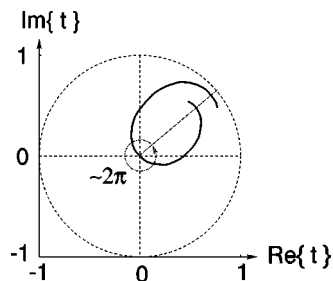


FIG. 5. Schematic representation of the path of the transmission amplitude as a function of the particle energy for the case that there is a transmission zero. The energy interval covered is that needed for the transition from one resonant peak (in the transmission probability) to the next resonant peak. The phase changes by about 2π .

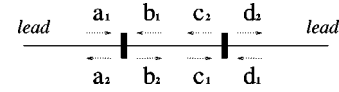


FIG. 6. Current amplitudes in the double-barrier model.

Aharonov-Bohm effect in a two terminal geometry is *out of phase* on consecutive resonant peaks, whereas for a scatterer of type *B* (see Fig. 5), the Aharonov-Bohm oscillations are *in phase*. With respect to the experiment of Yacoby *et al.*, it is an in-phase behavior that is needed to explain the data.

IV. EXAMPLES

In this section we present the calculations that lead to Figs. 1, 2, and 3 for the transmission amplitude. In addition we present results for the density of states as a function of energy that we compare with the transmission probability.

A. The resonant double barrier

The first example is a one-dimensional double-barrier model, which consists of two consecutive potential barriers that scatter particles moving along the x axis. A schematic illustration is shown in Fig. 6.

We assume that the two potential barriers in this model are identical and that each potential barrier is symmetric with respect to particles incident from the left and the right. The current amplitudes a_j , b_j , c_j and d_j , $j=1,2$, which are shown in Fig. 6, are connected by the relations

$$\begin{pmatrix} a_2 \\ b_2 \end{pmatrix} = \begin{pmatrix} \tilde{r} & \tilde{t} \\ \tilde{t} & \tilde{r} \end{pmatrix} \begin{pmatrix} a_1 \\ b_1 \end{pmatrix}, \quad (15)$$

$$\begin{pmatrix} c_2 \\ d_2 \end{pmatrix} = \begin{pmatrix} \tilde{r} & \tilde{t} \\ \tilde{t} & \tilde{r} \end{pmatrix} \begin{pmatrix} c_1 \\ d_1 \end{pmatrix}. \quad (16)$$

Here \tilde{r} and \tilde{t} are the reflection and the transmission amplitude of the potential barriers, respectively. The amplitudes in the well are related by $b_1 = \tau c_2$ and $c_1 = \tau b_2$, where $\tau = \exp(i\varphi)$ is the transmission amplitude of the well and φ the phase accumulated by a one time traversal of the well.

We have to find the scattering matrix S that relates the outgoing current amplitudes a_2, d_2 to the incoming current amplitudes a_1, d_1 . A little algebra gives

$$S = \begin{pmatrix} \tilde{r} & 0 \\ 0 & \tilde{r} \end{pmatrix} + \frac{\tilde{t}^2 \tau}{1 - \tilde{r}^2 \tau^2} \begin{pmatrix} \tilde{r} \tau & 1 \\ 1 & \tilde{r} \tau \end{pmatrix}. \quad (17)$$

To proceed, we parametrize the scattering matrix of the single barrier also in terms of angular variables [see Eq. (4)]. We take $\tilde{r} = ie^{i\tilde{\theta}} \sin \tilde{\phi}$ and $\tilde{t} = e^{i\tilde{\theta}} \cos \tilde{\phi}$ with real angles $\tilde{\theta}$ and $\tilde{\phi}$. In our model the potential is uniform (except for the two barriers), and φ is thus connected to the energy E of a scattering particle via $\varphi = kl$, where l is the distance between the potential barriers and $k = \sqrt{2mE}/\hbar$ is the wave vector of the particle away from the barriers. We assume that the quantities $\tilde{\theta}$ and $\tilde{\phi}$ are independent of the energy E . This

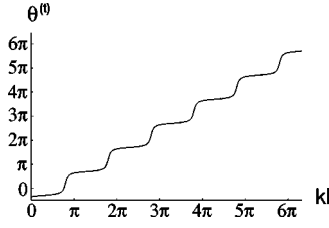


FIG. 7. Phase of the transmission amplitude as a function of $kl(=l\sqrt{2mE}/\hbar)$ for the double-barrier model.

implies, in particular, that there is no particle density inside each potential barrier. With these specifications the transmission amplitude t is given by

$$t = \frac{e^{i(kl+2\tilde{\theta})} \cos^2 \tilde{\phi}}{1 + e^{2i(kl+\tilde{\theta})} \sin^2 \tilde{\phi}}. \quad (18)$$

The transmission amplitude is a function of energy only through the energy dependence of the wave vector k . This result is used to give the transmission amplitude in the complex plane as a function of energy in Fig. 1. The parameters chosen for Fig. 1 are $\tilde{\theta}=2.2$ and $\tilde{\phi}=2.1$.

B. Phases and density of states in the double-barrier model

For comparison with the wire connected to a side branch, we now examine the phases in the double-barrier scattering problem and the density of states. To find the Friedel phase, we use Eq. (7) and find from Eq. (17),

$$\frac{\partial \theta^{(f)}}{\partial E} = \frac{\partial \varphi}{\partial E} \frac{1 - |\tilde{r}|^4}{|1 - \tilde{r}^2 \tau^2|^2}. \quad (19)$$

The derivative of the phase $\theta^{(t)}$ of the transmission amplitude is found from $\tan \theta^{(t)} = \text{Im}\{t\}/\text{Re}\{t\}$,

$$\frac{\partial \theta^{(t)}}{\partial E} = \left\{ 1 + \left(\frac{\text{Im}\{t\}}{\text{Re}\{t\}} \right)^2 \right\}^{-1} \frac{\partial \text{Im}\{t\}}{\partial E \text{Re}\{t\}}. \quad (20)$$

Substituting Eq. (18) into Eq. (20), we can show that for the resonant double barrier the derivatives of the two phases are identical,

$$\frac{\partial \theta^{(t)}}{\partial E} = \frac{\partial \theta^{(f)}}{\partial E}. \quad (21)$$

This result just restates Eq. (11) for the double-barrier model. The phase $\theta = \theta^{(t)} = \theta^{(f)} - \pi/2$ for the double-barrier model as a function of kl (wave vector times well width) is shown in Fig. 7. The specific parameters are $\tilde{\theta}=2.2$ and $\tilde{\phi}=2.1$. Thus, the phase shows a steplike behavior. It is nearly constant as a function of k and increases sharply when k , or the energy $E = \hbar^2 k^2 / (2m)$, coincides with a resonant state. To show this, we now examine the density of states.

For a perfect one-dimensional wire, the density of states per unit length and in a small interval of wave vectors is $dn/dk = 1/(2\pi)$ for carriers moving to the right. Since $dE/dk = \hbar v$, where v is the velocity of the carrier, the density of states per unit length and in a small energy interval is $\nu \equiv dn/dE = 1/(h v)$. We are interested in the density of states in the region between the two barriers. Denoting the

scattering states with unit amplitude of incident carriers from the left by $\Phi_1(x)$ and the scattering state of carriers with unit amplitude of carriers incident from the right by $\Phi_2(x)$, the local density of states can be expressed by³²

$$\nu(x) = \sum_{\mu=1}^2 \frac{1}{h v} |\Phi_{\mu}(x)|^2. \quad (22)$$

The density of states in the well region (between the two barriers) is the integral over the local density of states $\rho = \int_{-l/2}^{l/2} dx \nu(x)$. With an explicit calculation of the scattering states, we obtain

$$\rho = \frac{2l}{h v} \left| \frac{\tilde{t}}{1 - \tilde{r}^2 \tau^2} \right|^2 \left(1 + |\tilde{r}|^2 + 2 \text{Re}\{\tilde{r}\tau\} \frac{\sin \varphi}{\varphi} \right). \quad (23)$$

Here, for simplicity, we assume that the phase increment of a barrier traversal is zero. We have considered here the density of states that are obtained in terms of energy derivatives of phases or scattering matrices (as is widely done). Such derivatives do not naturally lead to an answer for a spatially local density of states. The density of states in the region between the two barriers is, however, a local question. A rigorous procedure to obtain local densities is via derivatives of phases and scattering matrices with respect to local potentials.⁸ The discussion given here (in terms of energy derivatives) is correct only up to WKB-like corrections. The last term in Eq. (23) contains a factor $1/(kl)$ and is thus small for wells that are much larger than a wavelength. Neglecting this term, we obtain

$$\bar{\rho} = \frac{2l}{h v} \frac{1 + \sin^2 \tilde{\phi}}{\cos^2 \tilde{\phi} + 4 \tan^2 \tilde{\phi} \cos^2(\tilde{\theta} + kl)}. \quad (24)$$

As is well known, for the case of opaque barriers ($\tilde{\theta} \rightarrow \pi/2$ and $\tilde{\phi} \rightarrow \pi/2$), the density of states becomes a series of delta functions $\lim_{\tilde{r} \rightarrow -1} \bar{\rho} = \sum_{n=1}^{+\infty} \delta(E - \pi^2 \hbar^2 n^2 / (2ml^2))$ that coincide with the peaks of perfect transmission. For wells much wider than the wavelength, we find from Eq. (24) that the peaks in the density of states are at the energies

$$E_n = \frac{\pi^2 \hbar^2}{2ml^2} \left[n - \frac{1}{\pi} \left(\tilde{\theta} - \frac{\pi}{2} \right) \right]^2. \quad (25)$$

Here n takes any integer value larger than $(2\tilde{\theta} - \pi)/2\pi$. Comparison of Eq. (19) with Eq. (24), leads to $\partial \theta^{(f)}/\partial E = \pi \bar{\rho}$, i.e., the Friedel sum rule in the double-barrier model.

Using Eqs. (18) and (24), we obtain

$$|t|^2 = \frac{|\tilde{t}|^2}{1 + |\tilde{r}|^2} \frac{\pi \hbar v \bar{\rho}}{l}, \quad (26)$$

a relation between the density of states $\bar{\rho}$ and the transmission probability $|t|^2$. This relation implies that the energy values E_n that determine the peaks in the transmission probability coincide with the energies E_n of the peaks in the density of states. Using this fact and Eq. (24), we can show

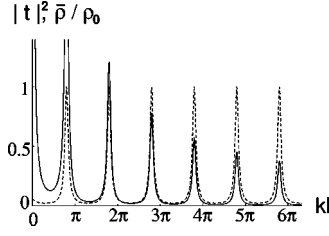


FIG. 8. Transmission probability (dashed line) and the density of states $\bar{\rho}$ (solid line) in units of $\rho_0 \equiv ml^2/(\pi\hbar^2)$ as a function of $kl (= l\sqrt{2mE}/\hbar)$ for the double barrier.

$$\int_{\varepsilon_n}^{\varepsilon_{n+1}} dE \bar{\rho} = 1. \quad (27)$$

In particular, Eq. (13) applies to the resonant double barriers with well widths large compared to the wavelength. Figure 8 shows the transmission probability and the density of states as a function of kl for the double barrier for the parameters $\bar{\theta}=2.2$ and $\bar{\phi}=2.1$. We emphasize this behavior of the double barrier, since, as we show in the next section, a wire with a side branch exhibits a transmission probability and a density of state that do not peak at the same energy.

C. Wire with a side branch

The second example that we investigate is a perfect one-dimensional wire with a side branch, which we also call the ‘‘stub’’ model. Such models have already a long history. The conductance of a wire with a side branch was investigated in Refs. 33, 34, and 35. References 36, 37, and 38 considered charging effects in structures with side branches. The parity of such closed structures is discussed in Refs. 37 and 39. In the context of the present work, the phase behavior of the transmission amplitude was investigated by Singha Deo and Jayannavar^{18,40,41} and Ryu and Cho.²³ However, neither of these two works makes the distinction between the Friedel phase and the phase of the transmission amplitude. Below, we investigate these two phases for a perfect wire to which a side branch of length l' is attached. A schematic illustration of this system is shown in Fig. 9.

The junction between the wire and the side branch is described by a wave splitter.^{42,43} We consider the time-reversal invariant case only and consider a splitter, which is symmetric with respect to carriers incident from the left and right lead. Furthermore, we assume the potential away from the junction is the same in all branches. The current amplitudes a'_j , b'_j , and c'_j , $j=1,2$, which are shown in Fig. 9, are connected by the relations

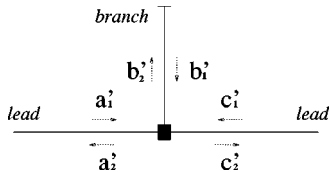


FIG. 9. Current amplitudes for the model of a wire with a side branch.

$$\begin{pmatrix} a'_2 \\ b'_2 \\ c'_2 \end{pmatrix} = \begin{pmatrix} \tilde{r}' & \varepsilon & \tilde{t}' \\ \varepsilon & \sigma & \varepsilon \\ \tilde{t}' & \varepsilon & \tilde{r}' \end{pmatrix} \begin{pmatrix} a'_1 \\ b'_1 \\ c'_1 \end{pmatrix}, \quad (28)$$

and $b'_1 = \tau' b'_2 \equiv e^{i\varphi'} b'_2$ with $\varphi' = 2kl' + \pi$. Here k is the wave vector of a particle with energy E . The constant π in φ guarantees that the wave function has a node at the upper end of the stub. In Eq. (28), \tilde{r}' is the reflection amplitude from a lead to itself, \tilde{t}' is the transmission amplitude from a lead to another lead, σ is the reflection amplitude from the stub to itself, ε is the transmission amplitude from a lead to the stub or from the stub to a lead, and τ' is the transmission amplitude by which the particle starting from the junction returns to the junction through the stub.

For the scattering matrix, relating the incident amplitudes in the wire a'_1, c'_1 to the out-going amplitudes a'_2, c'_2 in the wire (see Fig. 9), we obtain

$$S = \begin{pmatrix} \tilde{r}' & \tilde{t}' \\ \tilde{t}' & \tilde{r}' \end{pmatrix} + \frac{\varepsilon^2 \tau'}{1 - \sigma \tau'} \begin{pmatrix} 1 & 1 \\ 1 & 1 \end{pmatrix}. \quad (29)$$

Here the first matrix on the right-hand side arises from direct transmission past the side branch and direct reflection at the wave splitter due to the side branch, whereas the second term on the right-hand side is the contribution due to carriers that enter the stub and thus undergo a multiple-scattering process. We assume that the scattering amplitudes \tilde{r}' , \tilde{t}' , σ , and ε are real numbers, $\varepsilon \neq 0$, and are independent of the energy E . These assumptions, and the fact that the scattering matrix (28) must be unitary, demands⁴³

$$\tilde{r}' = (\lambda_1 + \lambda_2 \sqrt{1 - 2\varepsilon^2})/2, \quad (30)$$

$$\tilde{t}' = (-\lambda_1 + \lambda_2 \sqrt{1 - 2\varepsilon^2})/2, \quad (31)$$

$$\sigma = -\lambda_2 \sqrt{1 - 2\varepsilon^2}, \quad (32)$$

where λ_j is 1 or -1 ($j=1,2$). Depending on the choice of the λ 's, four different wave splitters are obtained. The value of the coupling constant ε is in the interval $[-1/\sqrt{2}, 1/\sqrt{2}]$. Using such a wave splitter leads to a transmission amplitude

$$t = \frac{-\lambda_1 + \lambda_2 \sqrt{1 - 2\varepsilon^2}}{2} \frac{1 + \lambda_1 e^{2ikl'}}{1 - \lambda_2 \sqrt{1 - 2\varepsilon^2} e^{2ikl'}}. \quad (33)$$

The path of this amplitude in the complex plane as a function of energy is shown in Fig. 2 for the case $\lambda_1 = -1$. The path is a circle through the origin since Eq. (33) implies $|t + \lambda_1/2|^2 = 1/4$. From Eq. (33) it follows that the wire with the stub has zero points of the transmission probability at the energies

$$E^{(n)} = \frac{\pi^2 \hbar^2}{2ml'^2} \left(n - \frac{1 + \lambda_1}{4} \right)^2, \quad (34)$$

$n=1,2,\dots$. We re-emphasize that in contrast to the case of the double barrier the origin is included in the path of the transmission amplitude.

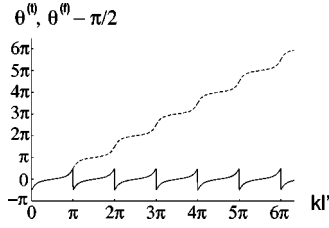


FIG. 10. Phase of the transmission amplitude $\theta^{(t)}$ (solid line) and Friedel phase $\theta^{(f)} - \pi/2$ (dashed line) as a function of kl' for the wire with the side branch.

D. Phases and density of states in wire with a side branch

Let us now investigate the Friedel phase and the phase of the transmission amplitude for the wire with a side branch. Using Eqs. (7) and (29), the derivative of the Friedel phase $\theta^{(f)}$ with respect to the energy E in the wire with a side branch is given by

$$\frac{\partial \theta^{(f)}}{\partial E} = \frac{\partial \varphi'}{\partial E} \left| \frac{\varepsilon}{1 - \sigma \tau'} \right|^2. \quad (35)$$

As shown in Sec. IV C, there are zero points in the transmission amplitude as a function of the energy in the stub model, so that abrupt phase changes of the transmission amplitude do occur. Thus, we need a limiting procedure to define the phase of the transmission amplitude. To this end, we add a small perturbation $\pm \eta$, $\eta > 0$ to the transmission amplitude

$$\bar{t}_{\pm} \equiv t \pm \eta \quad (36)$$

and evaluate the phase of \bar{t}_{\pm} in the limit $\eta \rightarrow +0$. The derivative of the phase $\theta^{(t)}$ of the transmission amplitude with respect to the energy E is thus given by

$$\frac{\partial \theta^{(t)}}{\partial E} = \lim_{\eta \rightarrow +0} \left\{ 1 + \left(\frac{\text{Im}\{\bar{t}_{\pm}\}}{\text{Re}\{\bar{t}_{\pm}\}} \right)^2 \right\}^{-1} \frac{\partial}{\partial E} \frac{\text{Im}\{\bar{t}_{\pm}\}}{\text{Re}\{\bar{t}_{\pm}\}}. \quad (37)$$

Using our specific result for the transmission amplitude, we obtain

$$\frac{\partial \theta^{(t)}}{\partial E} = \frac{\partial \theta^{(f)}}{\partial E} \pm \lambda_1 \pi \sum_{n=1}^{+\infty} \delta(E - E_n). \quad (38)$$

A detailed derivation of Eq. (38) is given in the Appendix. Figure 10 shows the phase of the transmission amplitude and the Friedel phase of the wire with a side branch as a function of kl' . We have chosen the branch of the wave splitter with $\lambda_1 = -1$, $\lambda_2 = 1$ and a coupling constant $\varepsilon^2 = 0.35$.

Let us next investigate the density of states. The wire is taken to be on the x axis, with the splitter located at $x = 0$. The stub points along the positive y axis. The splitter is described by an energy independent scattering matrix and can thus be viewed as pointlike. A scattering state of unit amplitude $\exp\{ik_{\mu}x\}$ describing particles incident from the μ th lead ($\mu = 1, 2$) gives in the side branch rise to a wave $\Psi_{\mu}(y)$. Here $k_1 = k$ for a wave incident from the left and $k_2 = -k$ for a wave incident from the right. The local density of states $\nu(y)$ in the side branch is given by $\nu(y) = \sum_{\mu=1}^2 |\Psi_{\mu}(y)|^2 / (h\nu)$, and the total density of states is

given by the integral of the local density of states over the entire length of the stub, $\rho = \int_0^{l'} dy \nu(y)$. We find

$$\rho = \frac{l'}{h\nu} \left| \frac{2\varepsilon}{1 - \sigma e^{i\varphi'}} \right|^2 \left(1 + \frac{\sin \varphi'}{\varphi' - \pi} \right). \quad (39)$$

In the WKB limit of interest here, for a side branch much longer than the Fermi wavelength, the second term in the bracket of the right-hand side of Eq. (39) can be neglected. Using Eq. (32), we obtain for a long side branch the density of states

$$\bar{\rho}' = \frac{l'}{h\nu} \frac{4\varepsilon^2}{(1 - \sqrt{1 - 2\varepsilon^2})^2 + 4\sqrt{1 - 2\varepsilon^2} \sin^2(K_2 l')}. \quad (40)$$

Here K_j , $j = 1, 2$ is defined by $K_j \equiv k + (1 - \lambda_j)\pi/(4l')$. For a stub much longer than a wavelength, the energies at which the density of states peaks are given by

$$E'_n = \frac{\pi^2 \hbar^2}{2ml'^2} \left(n - \frac{1 - \lambda_2}{4} \right)^2. \quad (41)$$

In the weak-coupling limit $\varepsilon \rightarrow +0$, using Eq. (40), we obtain $\lim_{\varepsilon \rightarrow +0} \bar{\rho}' = \sum_{n=1}^{+\infty} \delta(E - E'_n)$. Here the right-hand side is the density of states of a particle confined in the completely isolated stub but taking into account that the phase change at the closed coupler is as dictated by $\lambda_2 = 1$. The comparison of Eq. (35) with Eq. (40) leads to $\partial \theta^{(f)}/\partial E = \pi \bar{\rho}'$. We have thus verified the Friedel sum rule for the wire with a side branch.

Let us now show that in this scattering problem (for the splitters with $\lambda_1 \lambda_2 = -1$) the peaks in the transmission probability do not coincide with the peaks in the density of states. Using Eq. (33), the transmission probability $|t|^2$ can be expressed in the form

$$|t|^2 = \frac{(1 - \lambda_1 \lambda_2 \sqrt{1 - 2\varepsilon^2})^2 \cos^2(K_1 l')}{(1 - \lambda_1 \lambda_2 \sqrt{1 - 2\varepsilon^2})^2 + 4\lambda_1 \lambda_2 \sqrt{1 - 2\varepsilon^2} \sin^2(K_1 l')}. \quad (42)$$

Therefore, the energy values E_n , $n = 1, 2, \dots$, at which the transmission probability peaks are given by

$$E_n = \frac{\pi^2 \hbar^2}{2ml'^2} \left(n - \frac{1 - \lambda_1}{4} \right)^2. \quad (43)$$

We see that for $\lambda_1 \lambda_2 = -1$ (i.e., depending on the choice of the splitter) these energy values are not equal to the energies E'_n , $n = 1, 2, \dots$, which determine the peaks of the density of states. Indeed, using Eqs. (40) and (42), we obtain for the relation between density of states and the transmission probability

$$|t|^2 = \frac{1}{\lambda_1 \sigma} \left\{ \tilde{t}'^2 - \frac{\pi \hbar \nu \varepsilon^2}{2l'} \bar{\rho}' \right\}. \quad (44)$$

Using Eqs. (40) and (43), we can show that $\int_{E_n}^{E_{n+1}} dE \bar{\rho}' = 1$. This implies that the condition (13) is fulfilled also by a wire with a side branch. The different behavior, depending on the sign of $\lambda_1 \lambda_2$, is especially apparent in the weak-

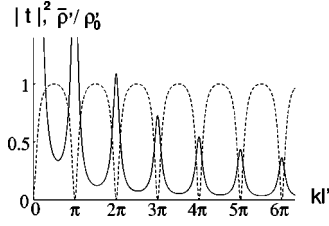


FIG. 11. Transmission probability (dashed line) and the density of states $\bar{\rho}'$ (solid line) in units of $\rho_0' \equiv ml'^2/(2\pi\hbar^2)$ for a wire with a side branch.

coupling limit. In this limit, for $\lambda_1\lambda_2 = -1$, almost all the particles incident from the wire on the wave splitter pass through the junction without noticing the side branch. Conversely, in the weak-coupling limit of a wave splitter with $\lambda_1\lambda_2 = 1$ almost all the particles incident from the wire on the wave splitter are reflected at the wave splitter. Figure 11 shows the transmission probability and the density of states as a function of kl' for the wire with a side branch connected by a junction with $\lambda_1 = -1$, $\lambda_2 = 1$, and $\varepsilon^2 = 0.35$.

E. Wire with scattering and a side branch

The previous two models are examples that demonstrate two different behaviors of the transmission amplitude in the complex plane. These different behaviors are illustrated by Figs. 4 and 5. Clearly, both of these models are very particular (nongeneric), and the question arises how the behavior exemplified by these two simple models shows up in more complicated structures. To examine this question, we now consider a structure that incorporates both the resonant double barrier and the side branch. A schematic illustration of this system is shown in Fig. 12.

We use the same potential barrier as in the resonant double-barrier structure and the same wave splitter as we used for the description of the wire with the side branch. Again, we will assume that the potential outside these scatterers is everywhere the same. In this model the current amplitudes a_j'' , b_j'' , c_j'' , d_j'' , and e_j'' , $j=1,2$, which are shown in Fig. 12 with the directions, are connected by the relations

$$\begin{pmatrix} a_2'' \\ b_2'' \end{pmatrix} = \begin{pmatrix} \tilde{r} & \tilde{t} \\ \tilde{t} & \tilde{r} \end{pmatrix} \begin{pmatrix} a_1'' \\ b_1'' \end{pmatrix}, \quad (45)$$

$$\begin{pmatrix} b_1'' \\ c_1'' \end{pmatrix} = \begin{pmatrix} 0 & \tau \\ \tau & 0 \end{pmatrix} \begin{pmatrix} b_2'' \\ c_2'' \end{pmatrix}, \quad (46)$$

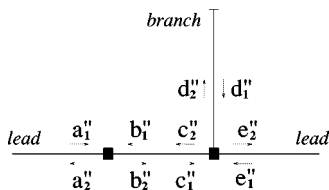


FIG. 12. Current amplitudes for a model with scattering in the wire and with a side branch.

$$\begin{pmatrix} c_2'' \\ d_2'' \\ e_2'' \end{pmatrix} = \begin{pmatrix} \tilde{r}' & \varepsilon & \tilde{t}' \\ \varepsilon & \sigma & \varepsilon \\ \tilde{t}' & \varepsilon & \tilde{r}' \end{pmatrix} \begin{pmatrix} c_1'' \\ d_1'' \\ e_1'' \end{pmatrix}. \quad (47)$$

Furthermore, as in the model with the side branch, we put $d_1'' = \tau' d_2''$.

For the overall scattering matrix of these systems, we obtain

$$S = \frac{1}{\tilde{r}^* D} \begin{pmatrix} V & W \\ W & -\lambda_1 \tau' \tau^2 V^* \end{pmatrix} \quad (48)$$

in which D , V , and W are defined by

$$D \equiv 1 - \sigma \tau' - \tilde{r} \tilde{r}' (1 + \lambda_1 \tau') \tau^2, \quad (49)$$

$$V \equiv D - |\tilde{t}|^2 (1 - \sigma \tau'), \quad (50)$$

$$W \equiv \tilde{r}^* \tilde{t}' (1 - \lambda_1 \tau') \tau. \quad (51)$$

The transmission amplitude t can be brought into the form

$$t = \frac{\tilde{t} \tilde{t}' (1 + \lambda_1 e^{2ikl'}) e^{ikl}}{1 + \sigma e^{2ikl'} - \tilde{r} \tilde{r}' (1 - \lambda_1 e^{2ikl'}) e^{2ikl}}. \quad (52)$$

In this representation the transmission amplitude t depends on the energy E only through the wave vector $k = \sqrt{2mE}/\hbar$. As a function of energy, the path of this transmission amplitude in the complex plane is shown in Fig. 3. Here the parameters chosen for Fig. 3 are $\tilde{\theta} = 2.2$, $\tilde{\phi} = 2.1$, $\lambda_1 = -1$, $\lambda_2 = 1$, $\varepsilon^2 = 0.35$, $l = 1$, and $l' = 4$. This figure shows clearly that a more general model combines the behavior of the resonant double-barrier model and the stub model. Sequences of turns of the transmission amplitude that path through the origin are interrupted by “double turns” characteristic of the resonant double barrier in which the transmission amplitude is nonzero. From Eq. (52), it can be noted that the wire with scattering and with a side branch has the same zero points for the transmission amplitude as the wire with the side branch.

V. CONCLUSIONS

In this work we have discussed the transmission amplitude as function of energy in the complex plane for scattering systems (without a magnetic field) connected to two single-channel leads. We emphasize that there are two phases that are of importance, namely the phase that appears in the Friedel sum rule and the phase of the transmission amplitudes. Except in special cases, these two phases are, in general, different. This important point has also been emphasized by Lee.²⁷ The two phases are different if the transmission amplitude exhibits an energy at which it is zero. At these energies the transmission amplitude phase and the Friedel phase acquire an additional difference given by $\pm \pi$. If the transmission amplitude exhibits no zero point between resonances, the variation of the phase from one resonant peak to another is close to π . If a zero point exists, the phase change between consecutive resonance peaks of the transmission probability is close to 2π . This difference is shown

clearly in the paths of the transmission amplitude in the complex plane.

For a sufficiently general model, we expect sequences of resonant peaks that are in phase (the phase increases by 2π) interrupted by peaks that are out of phase (the phase increases only by π as we go from one peak to the next). In terms of the parity of the Aharonov-Bohm effect, these imply sequences of peaks over which the parity is conserved. These sequences are interrupted by transitions that generate a flip in the parity. It is clearly desirable to investigate now a number of statistical questions: For example, for a fully chaotic quantum dot, one would like to find the ensemble-averaged density of zeros and compare this with the ensemble-averaged density of states. Furthermore, one would like to know if such a cavity exhibits correlations in the occurrence of zeros (long sequences of zeros interrupted by a flip in the parity), etc. Since the distribution of eigenvalues is known, random matrix theory likely gives an answer to these questions.

We add a remark on Fano resonances: Fano resonances arise due to the coupling of discrete states with continuous states. Such resonances also exhibit transmission zeros.^{44–46} Consequently, for such resonances the Friedel phase also does not coincide with the phase of the transmission amplitudes. The wire with a side branch investigated here also couples a set of discrete states with a continuum and thus provides for interfering transmission paths. However, the resonances in this case are not of the Fano type (as shown in Fig. 11) but rather Breit-Wigner resonances in the reflection probability.

In this work we considered only the case of a scatterer connected to two single-channel leads. For a *two terminal* structure with *multichannel* leads, it can be shown that the scattering matrix can always be brought into a basis, in which the transmission and reflection matrices are separately diagonal. Thus, such a multichannel problem can always be decomposed into single-channel problems of the type investigated here. Moreover, in the experimentally relevant case, the dot is connected to the arms of the ring via tunnel barriers. Thus, the transmission probabilities of the eigenchannels differ exponentially, and we can expect that it is only one of the channels that is relevant. Nevertheless, the question of what would actually be measured in a multichannel experiment requires additional analysis that we have not provided here. Still a different situation arises in *multiterminal* structures, experimentally investigated by Schuster *et al.*,¹² where the constraints on phases are much less stringent, and additional types of graphs, beyond those discussed here, might be realized.

It is very interesting to investigate the behavior of the transmission amplitude in the complex plane for variations in parameters other than the energy. For instance, we can ask about the path of the transmission amplitude if the AB flux increases by a flux quantum in a multiple connected geometry. The additional questions raised in this section clearly demonstrate that the investigation of the path of the transmission amplitude in the complex plane is an interesting avenue of future research.

ACKNOWLEDGMENTS

We are grateful to A. Levy Yeyati, M. Devoret, and D. Esteve for stimulating discussions. T.T. acknowledges the

support of the Swiss Federal government. M.B. was supported by the Swiss National Science Foundation.

APPENDIX: RELATION BETWEEN PHASES FOR THE WIRE WITH A SIDE BRANCH

In this appendix we outline the derivation of Eq. (38), which relates the Friedel phase and transmission amplitude phase for the wire with a side branch. First, using Eqs. (33) and (36), we find

$$\bar{t}_{\pm} = \frac{-\lambda_1 - \sigma}{2} \frac{1 - \lambda_1 e^{i\varphi'}}{1 - \sigma e^{i\varphi'}} \pm \eta. \quad (\text{A1})$$

The transmission amplitude t is dependent on the energy only through the quantity φ' , so that we obtain

$$\frac{\partial \theta^{(t)}}{\partial E} = \lim_{\eta \rightarrow +0} \frac{\partial \varphi'}{\partial E} \frac{\partial \arg\{\bar{t}_{\pm}\}}{\partial \varphi'}. \quad (\text{A2})$$

Using Eq. (A1) the derivative $\partial \arg\{\bar{t}_{\pm}\}/\partial \varphi'$ is found to be

$$\begin{aligned} \frac{\partial \arg\{\bar{t}_{\pm}\}}{\partial \varphi'} &= \left\{ 1 + \left(\frac{\text{Im}\{\bar{t}_{\pm}\}}{\text{Re}\{\bar{t}_{\pm}\}} \right)^2 \right\}^{-1} \frac{\partial}{\partial \varphi'} \frac{\text{Im}\{\bar{t}_{\pm}\}}{\text{Re}\{\bar{t}_{\pm}\}} \\ &= \frac{1}{2} \frac{1 - \sigma^2}{1 + \sigma^2 - 2\sigma \cos \varphi'} \\ &\quad \times \frac{\mp 2f_1(\sigma, \varphi')\eta + f_3(\sigma, \lambda_1, \varphi')}{2f_2(\sigma, \varphi')\eta^2 + (1 \mp 2\lambda_1 \eta)f_3(\sigma, \lambda_1, \varphi')} \\ &= \frac{1}{2} \frac{1 - \sigma^2}{1 + \sigma^2 - 2\sigma \cos \varphi'} \\ &\quad + \frac{1}{2} F \left(1 \mp 2\lambda_1 \eta, \lambda_1 \sigma, \varphi' + \frac{1 + \lambda_1}{2} \pi \right), \quad (\text{A3}) \end{aligned}$$

where the functions $f_1(x, y)$, $f_2(x, y)$, and $f_3(x, y, z)$ are defined by

$$f_1(x, y) \equiv 2x - (1 + x^2)\cos y, \quad (\text{A4})$$

$$f_2(x, y) \equiv 1 + x^2 - 2x \cos y, \quad (\text{A5})$$

$$f_3(x, y, z) \equiv (1 + xy)^2(1 - y \cos z), \quad (\text{A6})$$

and the function $F(x, y, z)$ is defined by

$$F(x, y, z) \equiv \frac{(1 - x^2)(1 - y^2)}{(1 - x)^2(1 - y)^2 + 2(1 + xy)(x + y)(1 + \cos z)}. \quad (\text{A7})$$

$F(x, y, z)$ has the following properties. First, it follows that

$$\lim_{x \rightarrow \pm 1 \pm 0} F(x, y, z) = \begin{cases} 0 & \text{in } z = (2n + 1)\pi \\ \mp \text{sgn}(1 - y^2) \times \infty & \text{in } z \neq (2n + 1)\pi, \end{cases} \quad (\text{A8})$$

$n = 0, \pm 1, \pm 2, \dots$. Second, it follows that

$$\begin{aligned}
& \int_{\lambda}^{\lambda+2\pi} dz F(x, y, z) \\
&= \frac{1}{i} \oint_C d\omega \frac{(1-x^2)(1-y^2)}{[(1+xy)\omega+x+y][(x+y)\omega+1+xy]} \\
&= \begin{cases} +2\pi & \text{in } 0 \neq |x+y| < |1+xy| \\ -2\pi & \text{in } |x+y| > |1+xy| \neq 0, \end{cases} \quad (\text{A9})
\end{aligned}$$

where λ is a real number and $\omega \equiv \exp(iz)$. C is the path running counterclockwise on the circle whose center is the origin and the radius is 1. Equations (A8) and (A9) lead to

$$\lim_{x \rightarrow 1 \pm 0} F(x, y, z) = \mp 2\pi \operatorname{sgn}(1-y^2) \sum_{n=-\infty}^{+\infty} \delta(z - (2n+1)\pi). \quad (\text{A10})$$

Using Eq. (34) and the inequality $E > 0$, we obtain

$$\delta\left(\varphi' + \frac{1+\lambda_1}{2}\pi - (2n+1)\pi\right) = \left(\frac{\partial\varphi'}{\partial E}\right)^{-1} \delta(E - E^{(n)}). \quad (\text{A11})$$

From Eqs. (A2), (A3), (A10), and (A11) we derive

$$\frac{\partial\theta^{(t)}}{\partial E} = \frac{\partial\varphi'}{\partial E} \left| \frac{\varepsilon}{1-\sigma\tau'} \right|^2 \pm \lambda_1 \pi \sum_{n=1}^{+\infty} \delta(E - E^{(n)}). \quad (\text{A12})$$

Using Eqs. (35) and (A12), we obtain Eq. (38).

- ¹R. G. Newton, *Scattering Theory of Wave and Particles* (Springer-Verlag, New York, 1982).
²J. Friedel, *Philos. Mag.* **43**, 153 (1952).
³J. S. Langer and V. Ambegaokar, *Phys. Rev.* **121**, 1090 (1961).
⁴D. C. Langreth, *Phys. Rev.* **150**, 516 (1966).
⁵R. Dashen, S.-K. Ma, and H. J. Bernstein, *Phys. Rev.* **187**, 345 (1969).
⁶F. Kassubek, C. A. Stafford, and H. Grabert, *Phys. Rev. B* **59**, 7560 (1999).
⁷E. Akkermans, A. Auerbach, J. E. Avron, and B. Shapiro, *Phys. Rev. Lett.* **66**, 76 (1991).
⁸T. Christen, *Phys. Rev. B* **55**, 7606 (1997); V. Gasparian, T. Christen, and M. Büttiker, *Phys. Rev. A* **54**, 4022 (1996).
⁹V. A. Gopar, P. A. Mello, and M. Büttiker, *Phys. Rev. Lett.* **77**, 3005 (1996).
¹⁰M. Büttiker and A. M. Martin cond-mat/9902320 (unpublished).
¹¹A. Yacoby, M. Heiblum, D. Mahalu, and H. Shtrikman, *Phys. Rev. Lett.* **74**, 4047 (1995).
¹²R. Schuster, E. Buks, M. Heiblum, D. Mahalu, V. Umansky, and H. Shtrikman, *Nature (London)* **385**, 417 (1997).
¹³A. Levy Yeyati and M. Büttiker, *Phys. Rev. B* **52**, R14 360 (1995).
¹⁴G. Hackenbroich and H. A. Weidenmüller, *Phys. Rev. Lett.* **76**, 110 (1996).
¹⁵C. Bruder, R. Fazio, and H. Schoeller, *Phys. Rev. Lett.* **76**, 114 (1996).
¹⁶A. Yacoby, R. Schuster, and M. Heiblum, *Phys. Rev. B* **53**, 9583 (1996).
¹⁷G. Hackenbroich and H. A. Weidenmüller, *Phys. Rev. B* **53**, 16 379 (1996).
¹⁸P. S. Deo and A. M. Jayannavar, *Mod. Phys. Lett. B* **10**, 787 (1996).
¹⁹Y. Oreg and Y. Gefen, *Phys. Rev. B* **55**, 13 726 (1997).
²⁰G. Hackenbroich and H. A. Weidenmüller, *Europhys. Lett.* **38**, 129 (1997).
²¹G. Hackenbroich, W. D. Heiss, and H. A. Weidenmüller, *Phys. Rev. Lett.* **79**, 127 (1997).

- ²²H. Xu and W. Sheng, *Phys. Rev. B* **57**, 11 903 (1998).
²³C.-Mo Ryu and S. Y. Cho, *Phys. Rev. B* **58**, 3572 (1998).
²⁴R. Baltin, Y. Gefen, G. Hackenbroich, and H. A. Weidenmüller, cond-mat/9807286 (unpublished).
²⁵K. Kang, *Phys. Rev. B* **59**, 4608 (1999).
²⁶H. Q. Xu (unpublished).
²⁷H.-W. Lee, *Phys. Rev. Lett.* **82**, 2358 (1999).
²⁸P. G. Silvestrov and Y. Imry, cond-mat/9903299 (unpublished).
²⁹R. Baltin and Y. Gefen cond-mat/9907205 (unpublished).
³⁰A. Levy Yeyati (private communication).
³¹C. J. B. Ford, A. B. Fowler, J. M. Hong, C. M. Knoedler, S. E. Laux, J. J. Wainer, and S. Washburn, *Surf. Sci.* **229**, 307 (1990); For related works, see G. Cernicchiaro, T. Martin, K. Hasselbach, D. Mailly, and A. Benoit, *Phys. Rev. Lett.* **79**, 273 (1997); S. Pedersen, A. E. Hansen, A. Kristensen, C. B. Sørensen, and P. E. Lindelof, cond-mat/9905033 (unpublished).
³²M. Büttiker, *IBM J. Res. Dev.* **32**, 63 (1988).
³³F. Sols, M. Macucci, U. Ravaioli, and K. Hess, *Appl. Phys. Lett.* **54**, 350 (1989).
³⁴S. Subramanian, S. Bandyopadhyay, and W. Porod, *J. Appl. Phys.* **68**, 4861 (1990).
³⁵Z.-an Shao, W. Porod, and C. S. Lent, *Phys. Rev. B* **49**, 7453 (1994).
³⁶M. Büttiker, *Phys. Scr.* **T54**, 104 (1994).
³⁷M. Büttiker and C. A. Stafford, *Phys. Rev. Lett.* **76**, 495 (1996).
³⁸P. Cedraschi and M. Büttiker, *J. Phys.: Condens. Matter* **10**, 3985 (1998).
³⁹P. Singha Deo, *Phys. Rev. B* **53**, 15 447 (1996).
⁴⁰P. Singha Deo and A. M. Jayannavar, *Phys. Rev. B* **50**, 11 629 (1994).
⁴¹P. Singha Deo, *Solid State Commun.* **107**, 69 (1998).
⁴²H.-L. Engquist and P. W. Anderson, *Phys. Rev. B* **24**, 1151 (1981).
⁴³M. Büttiker, Y. Imry, and M. Ya. Azbel, *Phys. Rev. A* **30**, 1982 (1984).
⁴⁴U. Fano, *Phys. Rev.* **124**, 1866 (1961).
⁴⁵J. U. Nöckel and A. D. Stone, *Phys. Rev. B* **50**, 17 415 (1994).
⁴⁶J. Goeres *et al.* (unpublished).